Parameterization of Ionospheric Height Variations by Antenna Pattern Synthesis Technique

Zeti Akma Rhazali[*1] *and Ahmad Faizal Mohd Zain*[2]

[1]Department of Electronics & Communication Engineering, College of Engineering, Universiti Tenaga Nasional, Km. 7, Jalan UNITEN-IKRAM, 43000 Selangor, Malaysia. zetiakma@uniten.edu.my

[2]Faculty of Science and Technology, Universiti Sains Islam Malaysia, 71800 Nilai, Negeri Sembilan, Malaysia. dr.afaizal@yahoo.com

Abstract

This paper introduces a new alternative in representing temporal ionospheric height of peak electron density, h_{max}, variations using array antenna parameters. The use of polar cyclic diagram based on antenna radiation pattern is proposed. The height variations are illustrated using arrays of two-element arrays with array spacing in the x-direction of $\lambda/8$, and phase of $\pi/3$, and with element spacing in the y-direction of $\lambda/4$, and phase of zero. The antenna equivalent model of peak height variations may complement the classical way of representing h_{max} temporal variations and acts as a signature to any ionospheric height of peak density variations. It constitutes the novelty of the study.

1. Introduction

Ionosonde data established large database in empirical-based ionospheric models. The data obtained by the ionosonde are displayed through ionograms. Thus, ionogram is a graph of the virtual height (reflection height) of the ionosphere against frequency, or simply an image of frequency versus time delay (virtual height) of high frequency echoes from the ionosphere recorded by an ionosonde [1]. Whatever definition holds, ionogram is a genuine depiction of the present ionospheric condition of the Earth. The information allows more accurate determination of the state of the upper atmosphere. The data are used to measure changes in the Earth's ionosphere due to space weather events.

Ionograms are often converted into electron-density profiles which illustrate the variations of electron density with height. The variations in densities and heights constitute to different state of ionosphere behavior. These parameters are used to outline the morphology of the ionosphere. The spatial and temporal trends of the ionosphere are drawn from the long data records and appropriate mathematical functions are used to represent the characteristic variation patterns. Fourier-type combination of cosine and sine functions is used to represent the diurnal variations while statistical analyses are used to represent the monthly and seasonal average conditions. Variability studies are performed to quantitatively justify the ionosphere behavior under different ionospheric conditions.

The method of visualization through ionograms, electron-density profiles, and graphs of temporal variations has been the best classical methods used to represent or describe the ionospheric condition. In addition, there are also other ways to represent the ionospheric characteristics parameters such as using numerical mappings, tomography graphs, and etc.

In this study, a new alternative in representing temporal ionospheric height of peak electron density variations are introduced using array antenna parameters. The approach is commonly referred as parameterization where some attributes of the function are parameterized in terms of antenna radiation characteristics. The ionospheric parameters in this form are easier to describe and also more justifiable for comparison.

2. Design Principle

The temporal plot of median peak density height variations is the basis. The monthly median is derived from the data of geo-magnetically quiet condition to eliminate the effects of geomagnetic disturbances ($\Sigma K_p \leq 24$, where ΣK_p is the sum of the eight 3-hour K_p indices for the day). Sample of the median diurnal h_{max} representation is shown in Fig. 1. The observation data is shown by a solid line and smoothed values are shown in dotted form. The monthly median diurnal pattern usually preserve the shape in all months throughout the year. The highest magnitude is observed in December solstice and March equinox months during noon-time [2]. Thus, the data of June 2006 is worthy to consider as the variability is the lowest and height variations are almost comparable to other equatorial regions. It is observed that the h_{max} diurnal pattern is a cyclic event that peaks during noon-time and dips around midnight.

978-1-4673-5225-3/14/$31.00 ©2014 IEEE

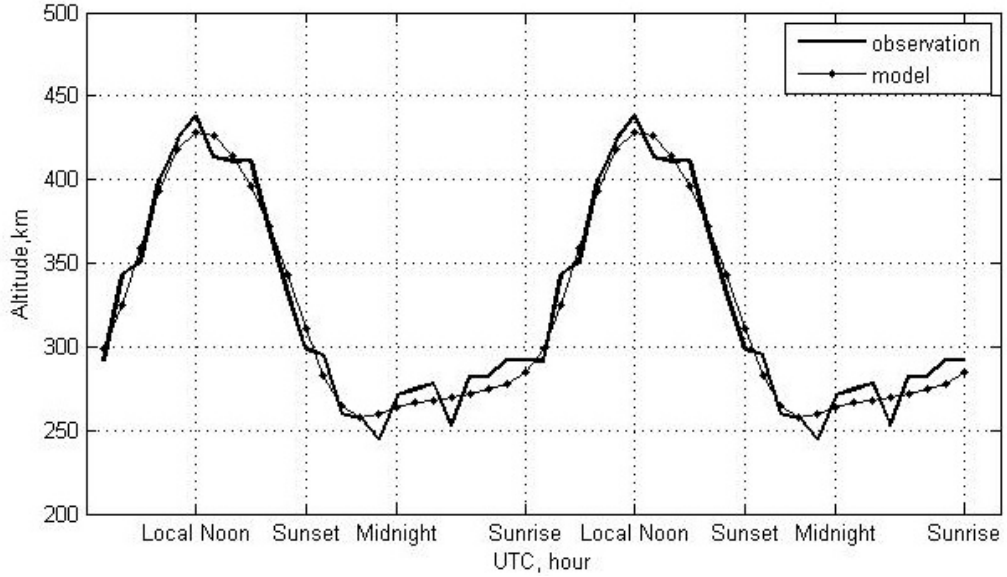

Figure 1. Median h_{max} of June 2006

Hence, the ionospheric height time variation can be represented into polar representation by appropriate transformation of the time domain. Using the relation,

$$\theta = \left(\frac{t}{T}\right) \times 2\pi \tag{1}$$

the time representation is transformed into polar representation. θ is the corresponding angle translated from time, t, and T is the number of hours in a day. In this case, T is a constant with value 24. Using equation (1), we get, for $t = 0$, $\theta = 0^o$; when $t = 12$, $\theta = 180^o$, and when $t = 24$, $\theta = 360^o$ or 0^o. The corresponding height are plotted accordingly. The new form of h_{max} variation is referred as polar cyclic diagram (as shown in Fig. 2).

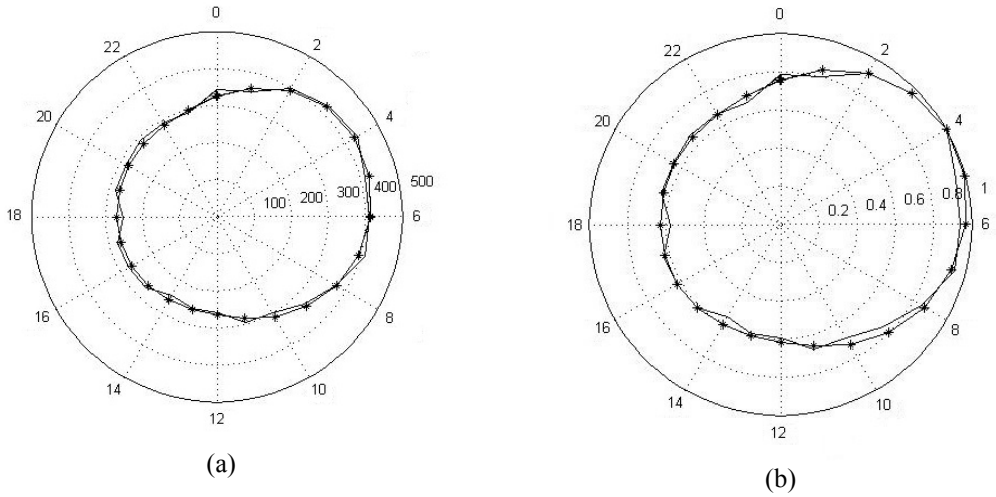

(a) (b)

Figure 2. Polar representation of h_{max} variations (a) unnormalized (b) normalized

3. Antenna Equivalence of Peak Height Variations

In this work, the new representation approximates an antenna radiation pattern similar to that of Fig. 3. The antenna has maximum gain in the main direction and lower gain at other directions. The antenna type and the excitation that produce the best approximation to the pattern is necessary to characterize the variations. In this work, array antenna is chosen as the characterisation technique based on the technical viability, simplicity and practicability.

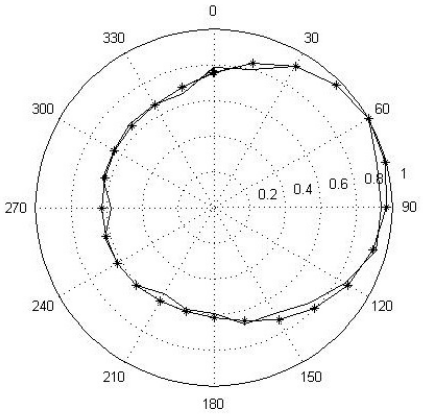

Figure 3. Antenna equivalence h_{max} variations radiation pattern

Considering the *N*-element linear array are isotropic point sources having uniform amplitudes and phases, equally spaced along the *x*-axis as an example, the normalized array factor, $f_n(\psi)$ is given as [3]

$$f_n(\psi) = \frac{\sin(N\psi/2)}{N\sin(\psi/2)} \approx \frac{\sin(N\psi/2)}{N\psi/2} \tag{2}$$

where

$$\psi = kd\cos\theta + \alpha \tag{3}$$

Equation (3) is the array phase function and is a function of the element spacing, d, phase shift, α, frequency, and elevation angle, θ. The maximum of the array factor occurs when the array phase function is zero. By changing these parameters the radiation characteristics of the array antenna may also change. Proper selection of N, d, and α ensures precise array pattern that matches the desired radiation pattern. Algorithms are written to determine the values of N, d, and α. There are many combinations of N, d, and α that are suitable for approximation. The array pattern from these combinations are compared with the desired radiation pattern (in this case is the antenna equivalence of peak height variations radiation pattern). Table 1 tabulates the results for different array configuration. Obviously, the array pattern of $N = 2$ with $d = \lambda/8$ for $\alpha = \pi/3$ is preferred as it has the greatest closeness of fit value. However the value can be further improved through pattern multiplication of two arrays.

Table 1. Closeness of fit results for different N, d, and α

N	***d***	***α***	**% fit**
2	$\lambda/4$	0	31
2	$\lambda/8$	0	31
2	$\lambda/3$	0	31
2	$\lambda/4$	$\alpha = \pi/3$	77
2	$\lambda/8$	$\alpha = \pi/3$	86
2	$\lambda/3$	$\alpha = \pi/3$	69
2	$\lambda/4$	$\alpha = \pi/6$	54
2	$\lambda/8$	$\alpha = \pi/6$	76
2	$\lambda/3$	$\alpha = \pi/6$	41

In this work, the pattern multiplication principle has been adapted whereby the isotropic point sources are being substituted with another array to form array of an array. The array factor for the entire array is then the product of the array factors of the array and can be written as:

$$\text{Total pattern} = \text{Array factor (2-element array)} \times \text{Array factor (2-element array)} \tag{4}$$

The array can be oriented such that the array elements are positioned along the same axis as the former array (co-linear array) or perpendicular to the axis of the former array (multidimensional array). Generally, the optimization of the array weights (amplitude and phase excitations) and array geometry (number of elements, element spacing) are necessary in seeking array patterns that accurately describe the desired radiation pattern. Both techniques are applied in this study. Anonymous results can be obtained. To precisely determine the optimum results, closeness of fit of the total array pattern to the desired pattern need to be performed.

Fig. 4 shows the pattern multiplication of two different arrays i.e., Array 1 is a two-element array with $d = \lambda/8$ and $\alpha = \pi/3$ while Array 2 is another two-element array with $d = \lambda/4$ and $\alpha = 0$. In Fig. 4(a), the arrays are co-linearly

positioned along the same axis. Array 1 has its main beam directed towards $\theta = 90^o$ while array 2 main beam is directed broadside to the array axis ($\theta = 0^o$, $\theta = 180^o$). Pattern multiplication of these array factors produced suppressed beam at their principle directions. In addition, when compared to the desired pattern, the offset is intolerable. Pattern multiplication of the array factors could result in a more accurate pattern if correct array configuration is used. Fig. 4(b) shows the result of the same arrays in (a) but oriented perpendicular to each other. From the graphical result, the array response fits well the desired radiation pattern compared to the former configuration. The total array pattern has its main beam directed at $\theta = 90^o$ and suppressed beam in other directions. In other word, the signal is amplified by constructive interference in the main direction whereby in other direction, the destructive interference has improve the beam sharpness. Hence, the viable configuration to approximate the desired pattern in the *x*-direction is $d_x = \lambda/8$, $\alpha_x = \pi/3$, and in the *y*-direction is $d_y = \lambda/4$, $\alpha_y = 0$. The closeness of fit has been improved by 10% using this technique.

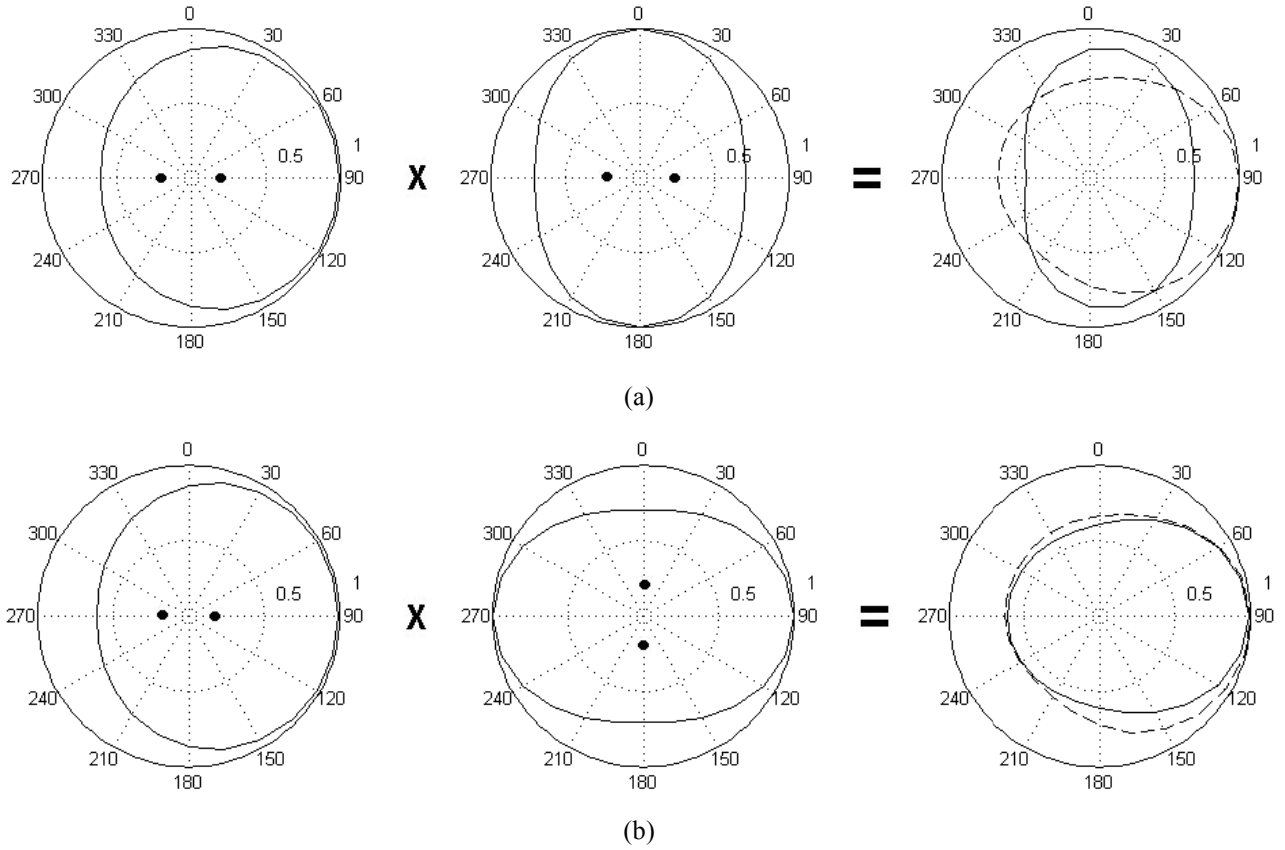

Figure 4. Pattern multiplication of two different arrays (a) linear configuration (b) multidimensional configuration. Array 1 is a two-element array with $d = \lambda/8$ and $\alpha = \pi/3$ while Array 2 is another two-element array with $d = \lambda/4$ and $\alpha = 0$. The total pattern (solid line) is compared to June 2006 antenna equivalence of peak height variations radiation pattern

4. Conclusion

It has been shown that the antenna equivalence of ionospheric height variations model is a new form of visualizing the ionospheric height variations. The model is a parameterized version of ionospheric height variations. The array of two-element arrays antenna is the signature of the height of peak electron density variations over Malaysia. The arrays are of non-uniform spacing with array spacing, $d_x = \lambda/8$, and element spacing, $d_y = \lambda/4$, while progressive phase shifts between arrays, $\alpha_x = \pi/3$, and progressive phase shift between elements, $\alpha_y = 0$. Both arrays have uniform amplitudes with the centre of the array located at the origin.

5. References

1. K. Davies, *Ionospheric Radio*, IEE Electromagnetic Wave Series 31. London, UK: Peter Peregrinus Ltd, 1990.

2. Z.A. Rhazali and A.F.M. Zain, "F-layer peak height variation near the equatorial anomaly crest during moderate solar activity,"*Proceeding of the 2013 IEEE International Conference on Space Science and Communication (IconSpace)*, 2013, pp. 424 - 428.

3. C.A. Balanis, *Antenna theory: analysis and design*, 2nded., John Wiley & Sons, Inc., USA, 1997.